minerals

Article

Metallogenic Model for Pb-Zn Deposits in Clastic Rocks of the Dahai Mining Area, Northeast Yunnan: Evidence from H-O-S-Sr-Pb Isotopes

Hongsheng Gong [1,2], Runsheng Han [1,2,*], Peng Wu [1,2], Gang Chen [1,*] and Ling Ma [3]

1 Faculty of Land Resources Engineering, Kunming University of Science and Technology, Kunming 650093, China; ghs7633@163.com (H.G.); wupeng8104@163.com (P.W.)
2 Southwest Institute of Geological Survey, Geological Survey Center for Non-ferrous Metals Resources, Kunming University of Science and Technology, Kunming 650093, China
3 City College, Kunming University of Science and Technology, Kunming 650093, China; maling@kust.edu.cn
* Correspondence: 11301124@kust.edu.cn (R.H.); chengang@kust.edu.cn (G.C.); Tel.: +86-139-8716-6018 (R.H.)

Abstract: The Dahai Pb-Zn mining area is located in the northwestern Pb-Zn district in northeastern Yunnan Province in the Sichuan-Yunnan-Guizhou Pb-Zn metallogenic triangle (SYGT), east of the Xiaojiang fault. Numerous Pb-Zn deposits (spots) occur in clastic rocks in this area. In this study, the Maliping, Laoyingqing, and Jinniuchang Pb-Zn deposits, representative clastic rocks in the Dahai mining area, were selected as research objects. The results of H-O-S-Sr-Pb isotope analyses show that the three deposits mainly formed through the mixing of a basinal brine with a hydrothermal fluid derived from deep within the underlying (deformed) basement, and brines leached organic matter from wall rocks. The $\delta^{34}S$ values range from −2.62–30.30‰. The S isotope results show two different sources of reduced S: one in the Laoyingqing deposit derived from the S reduction generated by the pyrolysis of sulfur-bearing organic matter in the carbonaceous slate of the Kunyang Group, and the second in the Maliping and Jinniuchang deposits derived from the S reduction generated by the thermochemical sulfur reduction (TSR) of seawater sulfate in the Lower Cambrian Yuhucun Formation and Sinian Dengying Formation. The Pb isotope results show that the Pb sources of the three deposits are derived from basement rocks (Kunyang Group) with a small portion derived from Devonian–Permian carbonate rocks and Dengying Formation dolomite, both of which have undergone homogenization during mineralization. The Sr content varied from 0.09629 to 0.2523×10^{-6}, and the study shows that the main source of Sr is a mixture of ore-forming fluid flowing through basement rocks (Kunyang Group) and through sedimentary cover. However, most of the Sr in the Maliping deposit is derived from marine carbonate, and in the Laoyingqing deposit, it is provided by basement rocks (Kunyang Group). Based on a comparative study of the deposits, the Pb-Zn deposits in the clastic rocks of the Dahai mining area and the SYGT belong to the same metallogenic system and were formed under the same metallogenic geological background. Finally, a unified metallogenic model of the two types of fluid migration and mixed mineralization of the Pb-Zn deposit in clastic rocks of the Dahai mining area is proposed. The metallogenic model provides a basis for the study of the Pb-Zn metallogenic system and guidance for deep and peripheral prospecting in this area.

Keywords: metallogenic model; H-O-S-Sr-Pb isotopes; Pb-Zn deposits in clastic rocks; Dahai Pb-Zn mining area; Sichuan-Yunnan-Guizhou Pb-Zn metallogenic triangle area; southwest China

Citation: Gong, H.; Han, R.; Wu, P.; Chen, G.; Ma, L. Metallogenic Model for Pb-Zn Deposits in Clastic Rocks of the Dahai Mining Area, Northeast Yunnan: Evidence from H-O-S-Sr-Pb Isotopes. *Minerals* **2023**, *13*, 1343. https://doi.org/10.3390/min13101343

Academic Editor: George M. Gibson

Received: 12 September 2023
Revised: 13 October 2023
Accepted: 13 October 2023
Published: 20 October 2023

1. Introduction

The Sichuan-Yunnan-Guizhou Pb-Zn metallogenic triangle (SYGT; including metallogenic areas in southwestern Sichuan, northeastern Yunnan, and southwestern Guizhou) occupies the core of the largest Pb-Zn base and the most promising metallogenic area in China. The metallogenic region of northeast Yunnan lies within the "triangle area" bordered by the Xiaojiang fault in the north-south direction, the Ziyun-Yadu fault in the northwestern direction, and the Mile-Shizong fault in the northeastern direction (Figure 1b). Most of the Pb-Zn deposits in this area occur in carbonate rocks and a small amount of siliceous carbonate in the Upper Sinian Dengying Formation, Devonian Zaige Formation, Carboniferous Baizuo and Weining formations, and Lower Permian Maokou Formation [1,2]. In recent years, many scholars have conducted in-depth research on the genesis, material source, metallogenic age, and metallogenic dynamic background of deposits in this area. Both Mississippi (MVT)- and sediment-dominated type deposits have been proposed [2–6]. Different sources have been proposed for the ore-forming material: (1) regional Mesoproterozoic basement rocks [4,7–9]; (2) carbonate strata and Emeishan basalt [2,10,11]; and (3) Mesoproterozoic basement strata and Sinian–Carboniferous sedimentary strata [12–15]. Therefore, the genesis and source of ore-forming materials of Pb-Zn deposits in this area remain controversial.

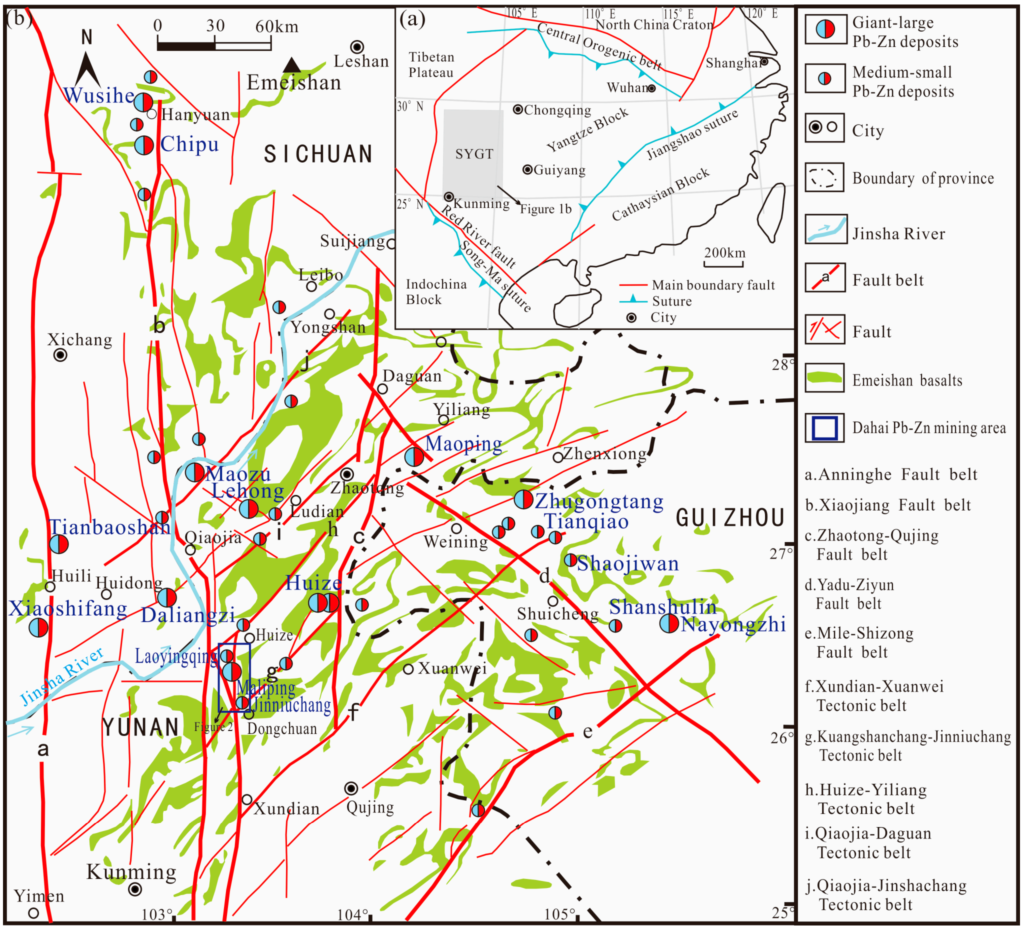

Figure 1. (**a**) Simplified tectonic map of south China [2]; (**b**) Distribution map of main faults and deposits in the Sichuan-Yunnan-Guizhou Pb-Zn metallogenic triangle area [2].

The Dahai Pb-Zn mining area is located in the northwestern metallogenic district in northeast Yunnan in the SYGT, east of the Xiaojiang fault. Numerous Pb-Zn deposits (spots) occur in clastic rocks in this area. Although few studies on the ore-forming material sources and metallogenic mechanism of Pb-Zn deposits in clastic rock in the SYGT have been conducted, whether the ore-forming material sources and metallogenic mechanism are consistent with those of other Pb-Zn deposits in the area remain to be deciphered. It is also directly related to the studies of the Pb-Zn metallogenic system and prospecting in the depth and periphery of the deposits in this area. Therefore, the large Maliping, small Laoyingqing, and Jinniuchang Pb-Zn deposits, which are representative of clastic rocks in the Dahai mining area, were selected for this study. Based on the analysis of the H, O, S, Sr, and Pb isotopic compositions, we traced the source of the ore-forming material, established a metallogenic model, and provided guidance for studies of the regional metallogenic mechanism. Based on the comparative analysis of the deposits, similarities, and differences in the sources of ore-forming material among the three deposits and other deposits in the area are revealed, providing guidance for the study of the Pb-Zn metallogenic system and prospecting in the depth and periphery of the deposits.

2. Regional Geology

The SYGT is located at the southwestern margin of the Yangtze Block (Figure 1a). The regional structure mainly develops several NS-trending faults supporting NE- and NW-trending secondary faults and folds [7]. Eight oblique strike-slip fault-fold belts controlled by NE-trending structures have mainly developed in the metallogenic district in northeast Yunnan [7] and have typical "polyhedral" structures (Figure 1b) [7].

Regional strata are mainly composed of basement and sedimentary cap rocks. Basement strata are mainly composed of Archean-Early Proterozoic crystalline and Mesoproterozoic folded basements [9]. The Kunyang Group (Huili Group) constitutes the fold basement, which consists of weakly metamorphosed marine volcanic and sedimentary rocks. Intrusive rocks are mainly distributed along the Anning River and Ganluo-Xiaojiang faults in a zonal manner. From south to north, they include the Jinning and Chengjiang granites, Hercynian layered basic-ultrabasic rocks, and Indosinian alkaline and acidic granites. Volcanic rocks from the Chengjiang Period are mainly intermediate-acidic intercalated basic volcanic and pyroclastic rocks and the Indosinian Period is characterized by the development of a large area of Emeishan basalts [12] with an eruption age ranging from 263 to 251 Ma [16].

The complex metallogenic structural system controls the widespread distribution of Pb-Zn deposits (Figure 1b). The Pb-Zn deposits in the metallogenic district in northeast Yunnan are mainly hosted in Mesoproterozoic epimetamorphic slate [17] and Neoproterozoic–Permian carbonate rocks. Layered, lenticular, and vein-shaped orebodies are controlled by oblique thrust fault zones.

3. Geology of the Dahai Mining Area

The Dahai Pb-Zn mining area is in the northwestern part of the metallogenic district in northeast Yunnan, adjacent to the east side of the SN-trending Xiaojiang fault. Faults and folds are well-developed in this area. NE-trending faults, including the Huize, Daibu, and Guancangqing faults, are the main structures in the area. Together with the SN-trending fault, they form the area's main structural framework and control the distribution direction of Pb-Zn (Ag) deposits (spots). EW-trending faults include the Qingmenkou fault. The main folds in the mining area are the NE-trending Wuxing anticline and Erdaoping syncline, SN-trending Shuicaozi syncline, and Pingqing inverted anticline. Exposed strata in the mining area include the Proterozoic Kunyang Group, Upper Sinian Dengying Formation, Early Paleozoic Cambrian strata, and Late Paleozoic Devonian–Triassic strata. Three types of magmatic rocks are exposed in the region: Variscan Permian Emeishan basalt (P_2), Variscan basic diabase and gabbro (υ), and Caledonian monzogranite (γ; Figure 2).

Pb-Zn deposits hosted in clastic rocks include the Laoyingqing, Maliping, and Jinniuchang deposits. The Maliping deposit is in the southwestern part of the NNE-trending Huize-Yiliang structural belt and is controlled by the Wuxing anticline. The orebody is in the interlayer detachment fracture zone at the interface of the siliceous cataclastic dolomite and clastic rock of the Lower Cambrian Yuhucun Formation. The degree of exploration is relatively high and large-scale resources have been identified. It is the largest Pb-Zn deposit with proven resources in this area. The roof of the orebody is clastic rock. The Yuhucun Formation is in the Sinian–Cambrian transition layer, which belongs to the continental shelf shallow sea sedimentary environment. Carbonate and clastic rock are alternately deposited, So the deposit is classified as a Pb-Zn deposit in clastic rocks. The Laoyingqing deposit is in the southwestern part of the NNE-trending Huize-Yiliang structural belt and is controlled by the Wuxing anticline. The orebody occurs in the interlayer detachment fracture zone of the carbonaceous slate (clastic rock) of the Kunyang Group. The Jinniuchang deposit is located in the SW part of the NE-trending Jinniuchang-Kuangshanchang structural belt and is controlled by the Daibu fault and Pingqing inverted anticline, which formed during the same period. The orebody occurs in the NWW-trending tensile fault zone of the siltstone of the Lower Cambrian Qiongzhusi Formation (Figure 2).

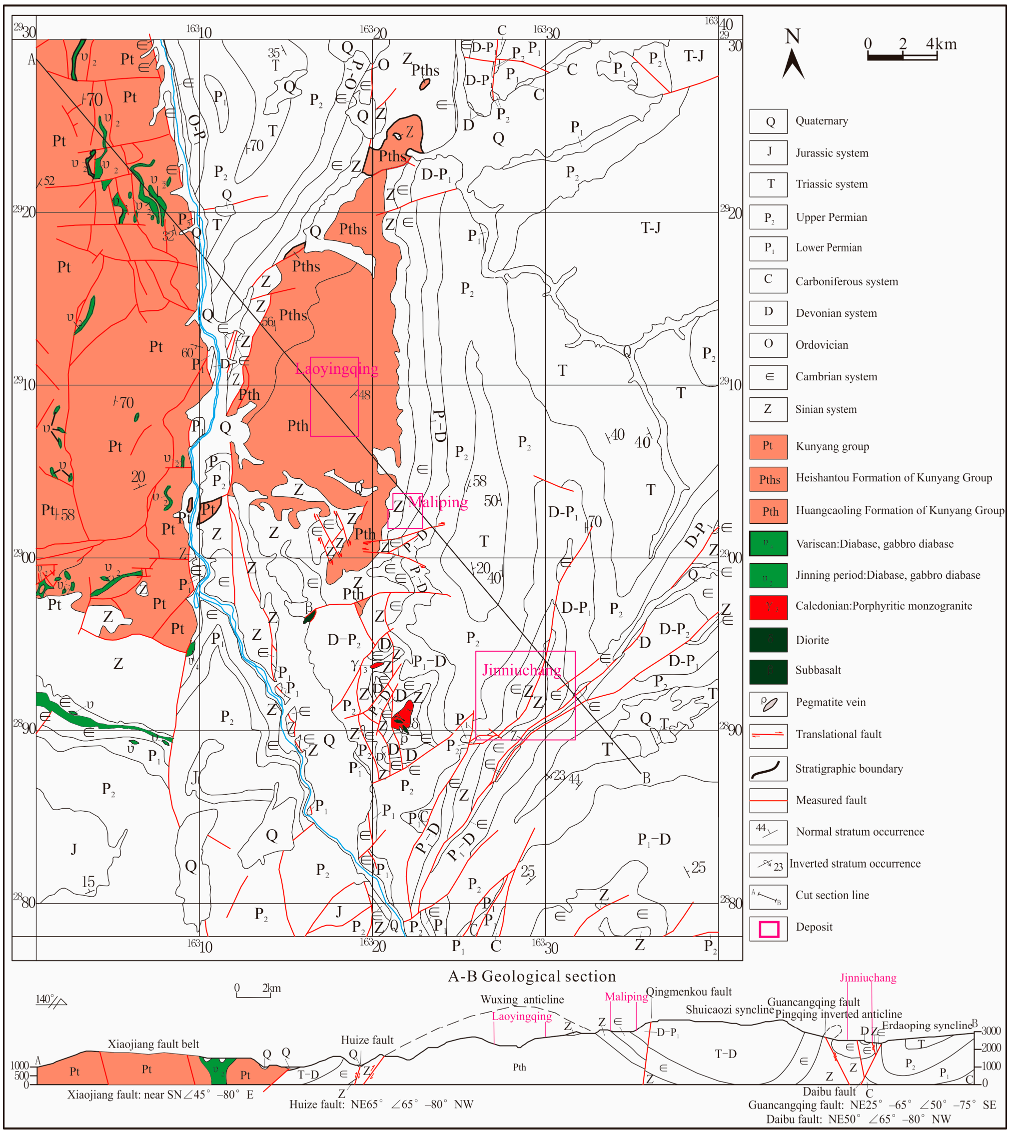

Figure 2. Geological map and geological section of Dahai Pb-Zn mining area.

Ore bodies can be seen in three forms: veins, stratiform, and lenticular. The ores consist mainly of sulfide, including sphalerite, galena, and pyrite; the gangue mineral is quartz. The ore texture mainly includes inclusion, mosaic, interstitial, automorphic, subhedral, and allomorphic granular structures. Ore structure types mainly include breccia, disseminated ore, banded ore, and veinlets (Figure 3).

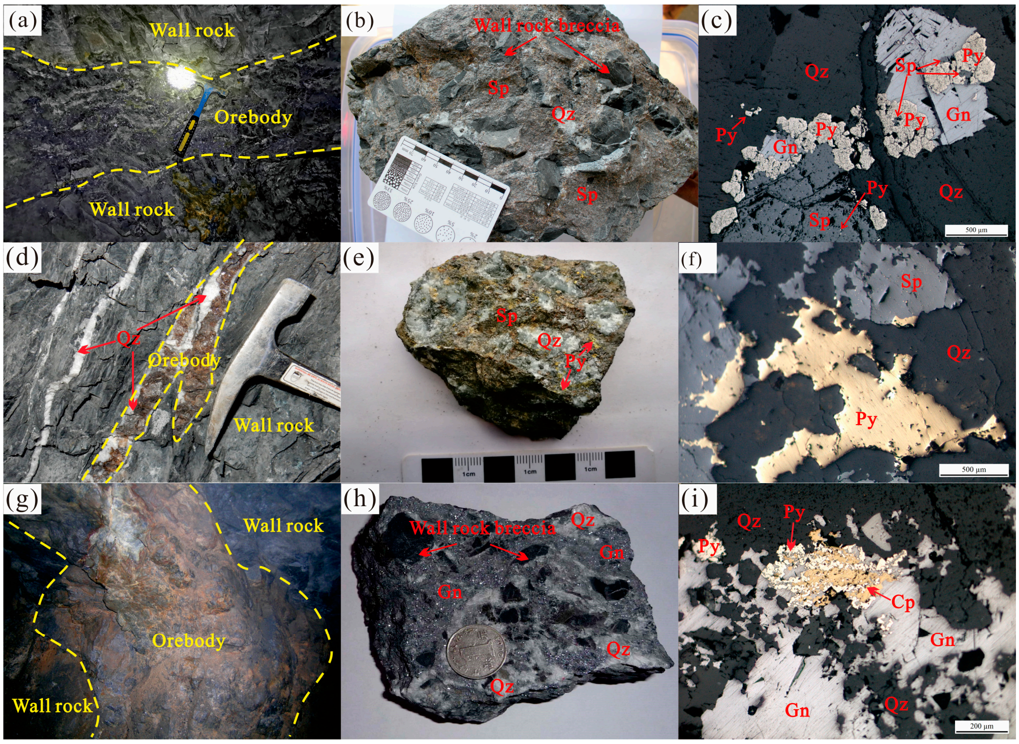

Figure 3. Characteristics of ore bodies and ore of Maliping, Laoyingqing, and Jinniuchang Pb-Zn deposits [17–19]. (**a**,**b**) stratiform orebody and breccia ore controlled by interlayer faults in Maliping Pb-Zn deposit; (**c**) pyrite and sphalerite coexist, galena metasomatic sphalerite and fine pyrite, and quartz metasomatic galena, sphalerite and fine pyrite; (**d**,**e**) vein orebody and breccia ore of the Laoyingqing Pb-Zn deposit; (**f**) quartz metasomatic sphalerite and coarse-grained pyrite, and pyrite is metasomatized by sphalerite; (**g**,**h**) stratiform orebody and breccia ore of Jinniuchang Pb-Zn deposit; and (**i**) fine pyrite metasomatic chalcopyrite, and quartz contains galena. (Sp—sphalerite; Gn—galena; Py—pyrite; Qz—quartz; Cp—chalcopyrite).

4. Sample Characteristics and Analysis Methods

4.1. Sample Collection

Eight representative primary metal sulfide ores were collected from different middle sections of the II-1 and II-2 ore bodies in the Maliping deposit. Six sphalerite, three pyrite, and three galena specimens were selected.

4.2. Analysis and Test Methods

The metal sulfide ore was crushed by hand and screened with a 40–60 mesh. Single crystals with high purity (>99%) were separated under a binocular lens and then analyzed.

The Rb-Sr isotopic tests were conducted at the Wuhan Geological Survey Center of the China Geological Survey (China). The sphalerite samples were washed three to five times with ultrapure water to remove salts. To avoid the influence of secondary inclusions, an appropriate amount of sample was ground with ultrapure water in a clean agate mortar. The fluid and residual phases were then separated by centrifugation. The fluid phase was diluted with a ^{85}Rb + ^{84}Sr mixed diluent and injected into an AG50W × 12 cation-exchange resin column, where Rb and Sr were desorbed. Finally, the Rb-Sr isotopic composition was analyzed on the solid-state mass spectrometer Triton (00682T). By analyzing the international standard NBS-987 to calibrate the Sr isotope instrumental fractionation. The standard 87Sr/86Sr measurement value is 0.710233 ± 6, which is consistent with the recommended value (0.71023 ± 5). The errors of 87Rb/86Sr and 87Sr/86Sr ratios (2σ) are 2% and 0.02%, respectively. For a detailed experimental process, please refer to Yang et al. [20].

S and Pb isotopic tests were conducted at Beijing Kehui Testing Technology Co., Ltd. (Beijing, China). For the S isotope analysis, a 253 Plus, Flash EA analyzer, and Conflo

IV multi-purpose interface were used. After the sample was fully burned, all generated gases were passed through a redox reaction tube filled with WO_3 and Cu wire to fully oxidize the gas. Pure SO_2 gas was obtained after passing through a chromatographic column and analyzed on the mass spectrometer. The three standard substances IAEA-S3, GBW04414, and GBW04415 were used in the experiment, and the analytical accuracy of the standard samples was better than 0.2‰. For the Pb isotope analysis, the F ion in the sample was removed by using HF + HNO_3, the sample was converted into chloride, and Pb was separated by the resin exchange method. Finally, Pb isotopes were measured using thermal surface ionization mass spectrometry. The background Pb of the entire process was 1×10^{-10} g. GV instruments IsoProbe-T and the static multi-receiving mode were used for the Pb isotope measurements.

5. Results

5.1. S Isotopic Composition

Ore sulfides in the Maliping deposit mainly include sphalerite, pyrite, and galena. The results of the S isotope analyses are shown in Table 1 and Figure 4a. Galena, sphalerite, and pyrite in the Maliping deposit are rich in heavy S isotopes, where the $\delta^{34}S$ values range from 8.25‰ to 30.30‰, with an average of 15.58‰. The $\delta^{34}S$ values of the six sphalerites vary from 8.25‰ to 13.20‰, with an average of 10.04‰. The $\delta^{34}S$ values of the three galena specimens range from 14.96‰ to 20.21‰, with an average of 16.80‰, and those of the three pyrites vary from 21.48‰ to 30.30‰, with an average of 25.45‰. The $\delta^{34}S$ of sphalerite is less than that of galena and the value obtained for galena is significantly less than that of pyrite (Figure 4a). The variation of the S isotope composition in the mining area is large, indicating that reduced S in the mining area may not be a single source.

Table 1. Sulfur isotopic compositions of sulfides in the Maliping, Laoyingqing, and Jinniuchang Pb-Zn deposit.

Deposit	Sample No./Quantity	Mineral	$\delta^{34}S$‰	Source
Maliping	MLP-1	Sphalerite	11.06	This paper
	MLP-2	Sphalerite	8.25	
	MLP-3	Sphalerite	8.98	
	MLP-5	Sphalerite	8.73	
	MLP-6	Sphalerite	10.03	
	MLP-7	Sphalerite	13.20	
	MLP-2-1	Galena	20.21	
	MLP-6-1	Galena	14.96	
	MLP-8-1	Galena	15.22	
	MLP-2-2	Pyrite	21.48	
	MLP-3-2	Pyrite	24.57	
	MLP-8-2	Pyrite	30.30	
Laoyingqing	7	Sphalerite	−2.62~1.42	[17]
	1	Pyrite	11.93	
Jinniuchang	7	Galena	9.34~20.70	[18]
	4	Pyrite	20.70~25.66	
	1	Sphalerite	21.49	

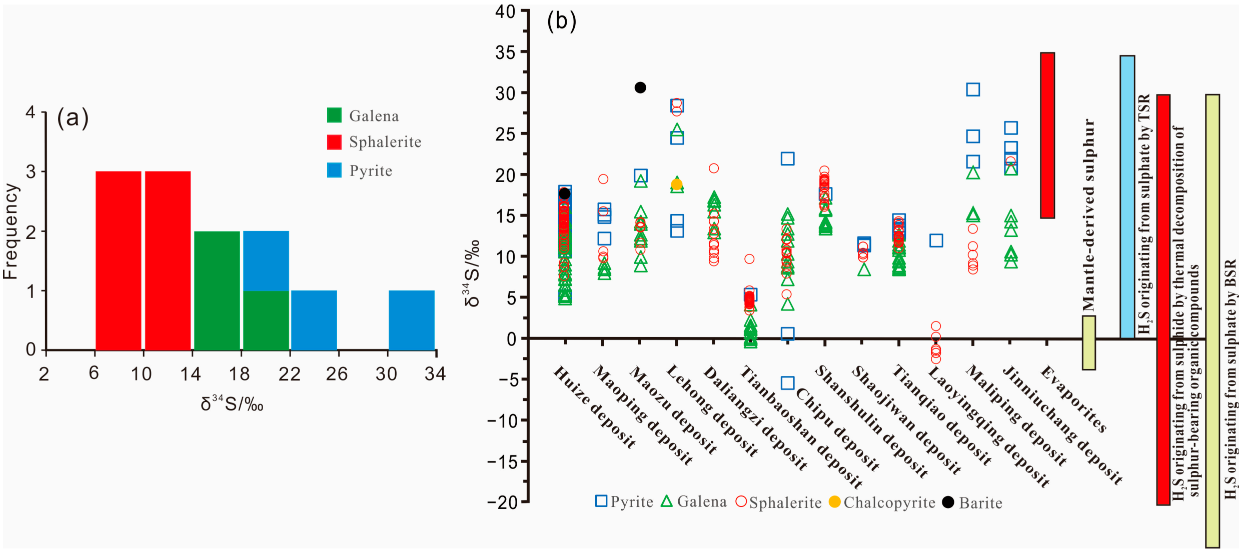

Figure 4. Histograms of the sulfur isotopic compositions of sulfides in the Maliping deposit (**a**) and Comparison of sulfur isotopic Compositions between the Maliping, Laoyingqing, and Jinniuchang Pb-Zn deposit and the major deposits in the SYGT [21] (**b**). (Huize [2,12,13,22]; Maoping [2,23]; Maozu [2,12,24]; Lehong [25]; Chipu [12,26]; Daliangzi [2,12,26,27]; Tianbaoshan [2,12,28–30]; Shanshulin [31]; Shaojiwan [32]; and Tianqiao [14]).

The S isotopic characteristics of the Maliping deposit are consistent with those of most Pb-Zn deposits in the SYGT, with $\delta^{34}S$ values ranging from 8 to 20‰ (Figure 4b).

5.2. Pb Isotopic Composition

The Pb isotopic compositions of the Maliping deposits are shown in Table 2. The $^{206}Pb/^{204}Pb$ values of ore sulfide in the Maliping deposit ranged from 17.8924 to 17.9927, with a range value of 0.0004. The $^{207}Pb/^{204}Pb$ values ranged from 15.6422 to 15.6616, with a range value of 0.0003. The $^{208}Pb/^{204}Pb$ values ranged from 37.9219 to 38.0572, with a range value of 0.0008.

Table 2. Pb isotopic compositions of sulfides in Maliping, Laoyingqing, and Jinniuchang Pb-Zn deposit.

Deposit	Sample No./Quantity	Mineral	$^{206}Pb/^{204}Pb$	2σ	$^{207}Pb/^{204}Pb$	2σ	$^{208}Pb/^{204}Pb$	2σ	Source
Maliping	MLP-1	Sphalerite	17.9612	0.0003	15.6480	0.0003	38.0070	0.0007	This paper
	MLP-2	Sphalerite	17.9927	0.0004	15.6557	0.0003	38.0572	0.0008	
	MLP-3	Sphalerite	17.9140	0.0004	15.6479	0.0003	37.9658	0.0008	
	MLP-5	Sphalerite	17.9497	0.0004	15.6539	0.0003	38.0128	0.0009	
	MLP-6	Sphalerite	17.9836	0.0005	15.6579	0.0004	38.0521	0.0010	
	MLP-7	Sphalerite	17.9897	0.0003	15.6567	0.0003	38.0528	0.0007	
	MLP-2-1	Galena	17.9849	0.0004	15.6554	0.0003	38.0329	0.0008	
	MLP-6-1	Galena	17.9834	0.0003	15.6574	0.0003	38.0504	0.0008	
	MLP-8-1	Galena	17.9549	0.0003	15.6616	0.0003	37.9931	0.0007	
	MLP-2-2	Pyrite	17.9222	0.0003	15.6480	0.0003	37.9682	0.0006	
	MLP-3-2	Pyrite	17.8924	0.0003	15.6422	0.0003	37.9219	0.0006	

Table 2. *Cont.*

Deposit	Sample No./Quantity	Mineral	$^{206}Pb/^{204}Pb$	2σ	$^{207}Pb/^{204}Pb$	2σ	$^{208}Pb/^{204}Pb$	2σ	Source
Laoyingqing	7	Sphalerite	17.9537~18.2907		15.6504~15.6755		37.9921~38.4494		[17]
	1	Pyrite	18.0048		15.6562		38.0799		
Jinniuchang	7	Galena	17.9513~17.9996		15.6499~15.6547		37.9893~38.0687		[18]
	4	Pyrite	17.9883~18.0081		15.6540~15.6571		38.0587~38.0918		
	1	Sphalerite	17.9996		15.6554		38.0741		

The Pb isotopic composition of the deposit is similar to that of the Chipu deposit, showing a narrow belt of linear horizontal extension within the Pb isotopic range corrected by the age of the basement rocks (Kunyang Group). It has been suggested that this feature is the result of the mixing of Pb from the Precambrian basement with secondary radiogenic Pb from overlying strata [33]. Other major Pb-Zn deposits in the SYGT mainly fall in the Pb isotope range of Devonian–Permian carbonate rocks and basement rocks and extend vertically (Figure 5a).

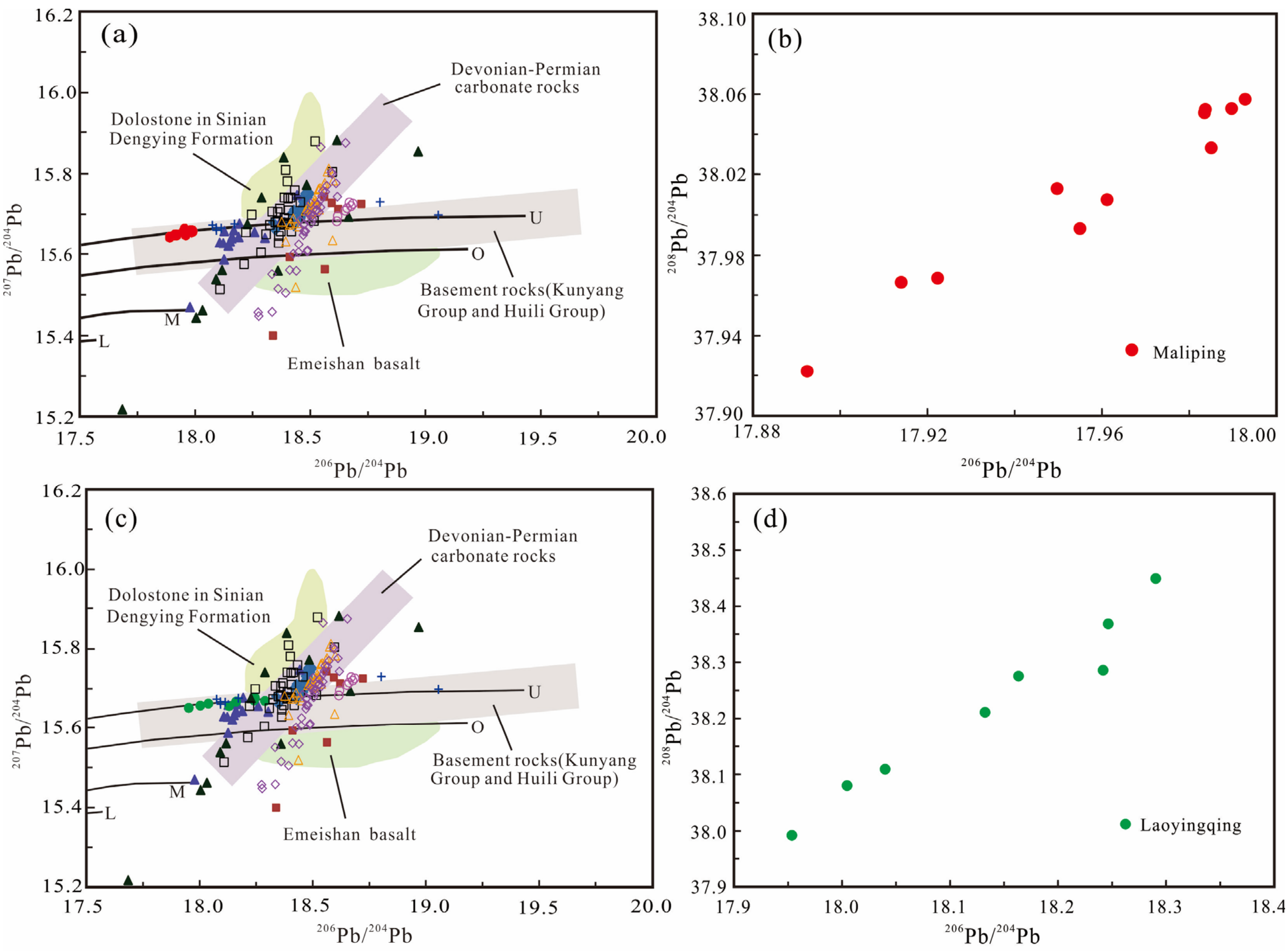

Figure 5. *Cont.*

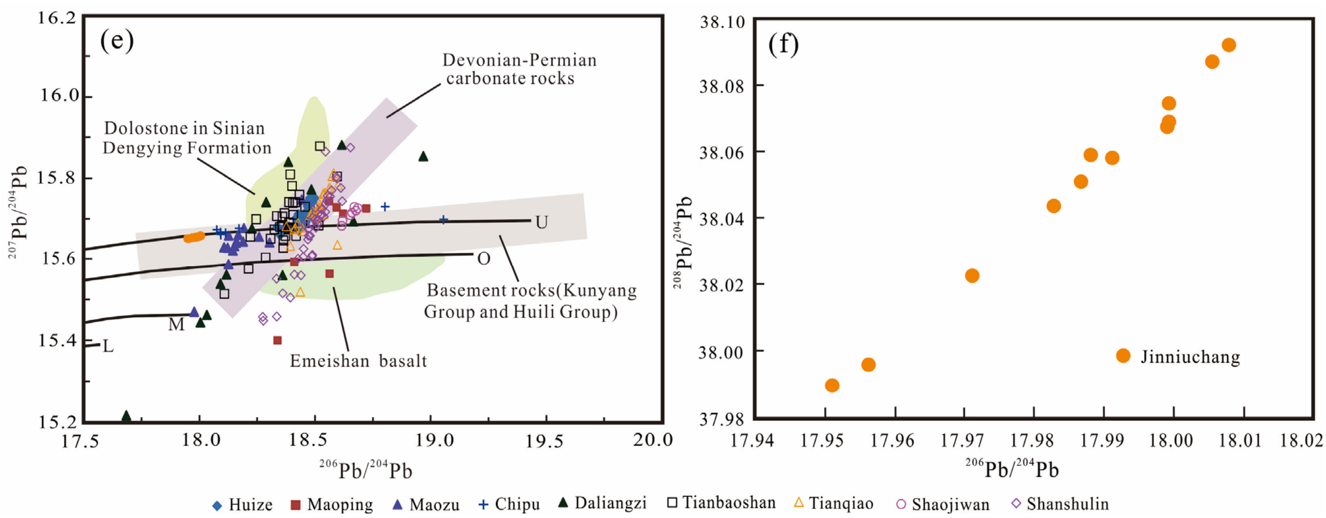

Figure 5. Plots of $^{207}Pb/^{204}Pb$ vs. $^{206}Pb/^{204}Pb$ for the Maliping, Laoyingqing, and Jinniuchang Pb-Zn deposit. (**a**,**c**,**e**) and Plots of $^{208}Pb/^{204}Pb$ vs. $^{206}Pb/^{204}Pb$ for the Maliping, Laoyingqing, and Jinniuchang Pb-Zn deposit (**b**,**d**,**f**). (Sinian Dengying Formation Dolostone, Devonian–Permian carbonate rocks, Basement rocks, and Emeishan basalt [1,2,4,8,22,34–38]; trends for the upper crust (U), orogen (O), mantle (M) and lower crust (L) are taken from Zartman and Doe [39]; Huize [40–42]; Maoping [2,23]; Maozu [2,24]; Chipu [26]; Daliangzi [43]; Tianbaoshan [28]; Tianqiao [14]; Shaojiwan [32]; and Shanshulin [31]).

5.3. Rb-Sr Isotope Results

The Rb-Sr isotopic analysis results obtained for the Maliping deposit are listed in Table 3. The Rb content of all sphalerite samples is relatively low (0.01294–0.0405 $\times$ 10^{-6}), the Sr content varied from 0.1407 to 0.2124 $\times$ 10^{-6}, the $^{87}Rb/^{86}Sr$ ratio ranged from 0.2652 to 0.6504 (mean 0.4186, n = 4), and the $^{87}Sr/^{86}Sr$ ratio varied from 0.71112 to 0.71597 (mean 0.71325, n = 4). The ideal Rb-Sr isochron age was not obtained because of the low Rb and Sr contents and the small variations in the $^{87}Rb/^{86}Sr$ and $^{87}Sr/^{86}Sr$ ratios.

Table 3. Sphalerite Rb-Sr isotopic compositions of the Maliping and Laoyingqing Pb-Zn deposit.

Deposit	Sample No./Quantity	Mineral	Rb/ppm	Sr/ppm	$^{87}Rb/^{86}Sr$	$^{87}Sr/^{86}Sr$	$(^{87}Sr/^{86}Sr)_{200Ma}$	Source
Maliping	MLP-5	Sphalerite	0.02822	0.2124	0.3832	0.71175 ± 0.00003	0.710677	This paper
	MLP-6		0.01294	0.1407	0.2652	0.71112 ± 0.00004	0.710377	
	MLP-7		0.02362	0.1816	0.3754	0.71414 ± 0.00004	0.713089	
	MLP-10		0.0405	0.1797	0.6504	0.71597 ± 0.00003	0.714149	
Laoyingqing	4	Sphalerite	0.01197~0.1335	0.09629~0.2523	0.3589~3.336	0.71950~0.72829	0.7184~0.7194	[17]

Remarks: $(^{87}Sr/^{86}Sr)t = {}^{87}Sr/^{86}Sr - {}^{87}Rb/^{86}Sr^{*}(e^{\lambda t}-1)$, $\lambda_{Rb} = 1.41 \times 10^{-11} t^{-1}$, t = 200 Ma.

The Rb-Sr isotopic compositions obtained for the Laoyingqing deposit are also listed in Table 3. The isochron age of sphalerite was determined to be 209.8 ± 5.2 Ma [17].

6. Discussion

6.1. S Source

The total S isotope composition of the hydrothermal solution during sulfide precipitation can be used to determine the S source of the deposit [44]. Barites and other sulfates are rare in the Maliping deposit, indicating a low oxygen fugacity. This indicates that the $\delta^{34}S$ value of ore sulfide represents the total S isotope composition of the hydrothermal solution and can be used to directly trace S sources [45].

The SN-trending Xiaojiang fault is a regional deep fault that provides channels at various locations for fluid circulation [7]. The Maliping deposit is east of the Xiaojiang fault and is located at the intersection of the Xiaojiang fault and NNE-trending Dongchuan-Wuxing-Luozehe structural belt. It is mainly controlled by the NE-trending Wuxing anticline. The main magmatic rocks in the Dahai mining area and SYGT are the Late Permian Emeishan basalt (~260 Ma) [46–50] and the basic diabase vein (156–166 Ma) [51]. The basalt formed before the regional metallogenic period (200 Ma) [52], whereas the diabase vein formed after the metallogenic period. Evidence for magmatism during the mineralization has not yet been found. Furthermore, systematic isotope studies (Pb-Sr) of the Maliping deposits do not support the participation of magmatic fluid (material) in mineralization. Therefore, it is less likely that the deep mantle-derived S(−3.0‰–+3.0‰) in this area participated in mineralization.

Gypsum, halite pseudocrystals, and bird's-eye dolomite have been reported in the Dengying Formation, which indicates gypsum salt deposition [53]. The $\delta^{34}S$ value of marine sulfate in the Sinian Dengying period of the Yangtze Block ranges from 20.0 to 38.7‰ [54], and the $\delta^{34}S$ value of marine sulfate in the phosphorites of the Lower Cambrian Meishucun Formation (Yuhucun Formation) ranges from 17.4 to 33.6‰ [55]. Marine sulfates can form reduced S through bacterial S reduction (BSR) and thermochemical S reduction (TSR) [56]. Generally, BSR occurs at relatively low temperatures (<120 °C, usually 50–70 °C) [57,58]. The S isotope fractionation generally varies from 4.0 to 46.0‰ and the $\delta^{34}S$ value of H_2S is typically negative [58]. However, TSR requires a relatively high temperature (>150 °C). At 150 °C, seawater sulfate can form a 10–25‰ fractionation with reduced S based on TSR, the $\Delta\delta^{34}S$ decreases with an increase in the temperature: at 150 °C, $\Delta\delta^{34}S$ = 15‰; at 200 °C, $\Delta\delta^{34}S$ = 10‰ [57,59,60]. However, S isotope fractionation between S in the metal sulfide and reduced S is not notable during sulfide precipitation. Therefore, in metal deposits, the $\delta^{34}S$ value of metal sulfide, with reduced S provided by TSR, should be 10–20‰ lower than that of seawater sulfate in the wall rock [26]. Studies on fluid inclusions in sphalerite and gangue minerals of several major deposits in the SYGT have shown that the homogenization temperature of the inclusions ranges from 115 to 280 °C, with an average range of 150–250 °C [17,18]. The average homogenization temperature of fluid inclusions from the Maliping deposit is 255 °C [19]. At this temperature, TSR may be the main mechanism responsible for the transformation of SO_4^{2-} into H_2S in the hydrothermal solution.

The $\delta^{34}S$ value of sulfides in the Maliping deposit ranges from 8.25 to 30.30‰, with an average of 15.58‰, which is lower than that of evaporites but very close to the S isotope fractionation caused by TSR. At the same time, the $\delta^{34}S$ value is very close to the average $\delta^{34}S$ value (generally 8–20‰) of most Pb-Zn deposits where reduced S is derived from the formation of seawater sulfate in the wall rock based on TSR [13,21,61–64] in the SYGT (Figure 4b). Therefore, reduced S in the deposit is mainly derived from the formation of seawater sulfate in the Lower Cambrian Yuhucun Formation in the wall rock and the underlying Sinian Dengying Formation based on TSR. The reduced S of the Jinniuchang deposit is mainly derived from the seawater sulfate in the underlying dolomite of the Lower Cambrian Yuhucun and Sinian Dengying formations based on TSR [18]. The S in the sulfides of the Laoyingqing deposit is mainly derived from the pyrolysis of S-bearing organic matter in the carbonaceous slate of the Kunyang Group [17], which is notably different from that of other Pb-Zn deposits in the SYGT (Figure 4b).

6.2. Sources of Ore-Forming Materials

6.2.1. Source of Ore-Forming Fluid

The H and O isotopic compositions of the Maliping, Laoyingqing, Jinniuchang, and the SYGT Pb-Zn deposits are listed in Table 4. Based on the δD-$\delta^{18}O_{water}$ relationship diagram (Figure 6), the analysis is as follows.

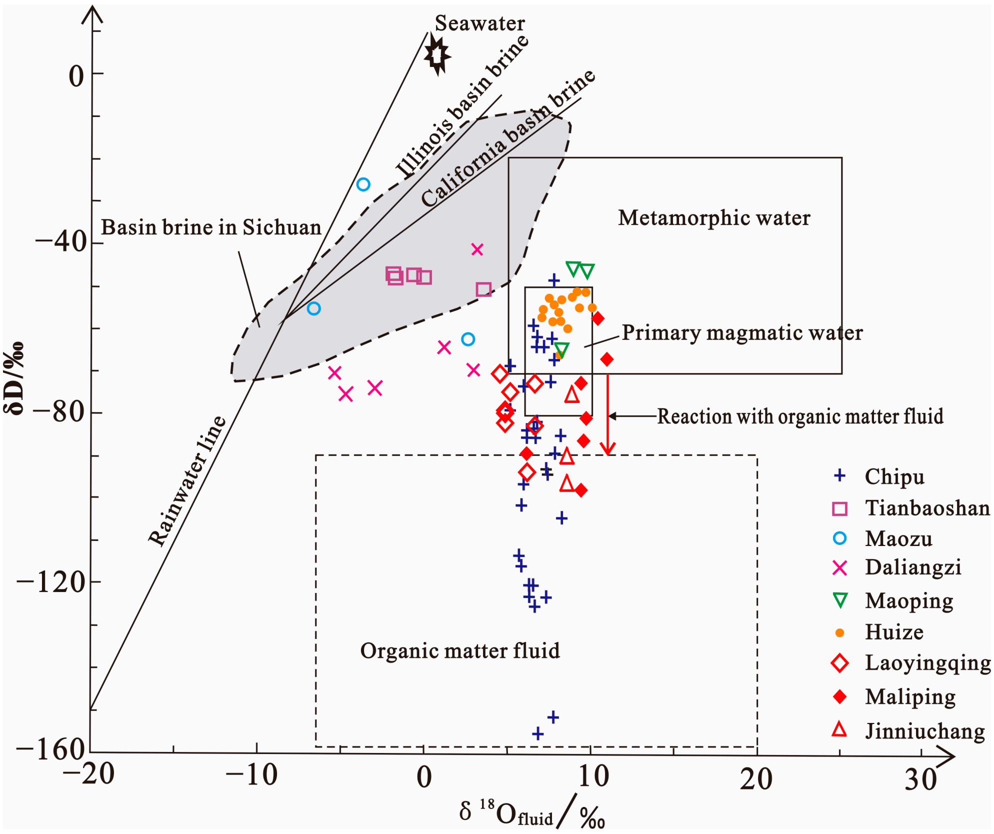

Figure 6. Diagram of δD vs.$\delta^{18}O_{fluid}$ for quartz separates from the Maliping, Laoyingqing, and Jinniuchang Pb-Zn deposits [65].

One sample from each of the three deposits falls within the range of primary magmatic water. However, magmatic rocks exposed in the Dahai mining area are mainly Permian Emeishan basalts, which are older than the mineralization and have much lower $^{87}Sr/^{86}Sr$ values than the ore (see discussion below). Therefore, it is unlikely that the ore-forming fluid is derived from magmatic water.

All H and O isotopes of quartz from the three deposits plot between metamorphic water and organic matter fluid. Combined with the structural ore control, these results suggest that ore-forming fluids are mainly derived from a mixture of tectonic-related fluids (tectonic fluids) and organic matter fluids, in addition to basin brine.

Sverjensky suggested that MVT-type Pb-Zn deposits are closely related to organic matter [66]. The lateral drift of $\delta^{18}O$ in the Maliping, Laoyingqing, and Jinniuchang deposits is small, whereas the δD value shows a greater vertical drift, which differs from the larger lateral drift of the $\delta^{18}O$ value of the MVT-type Tianbaoshan and Daliangzi Pb-Zn deposits but is similar to the δD-$\delta^{18}O$ characteristics of the Chipu Pb-Zn deposits, except for the δD variation range, which is smaller than that of the Chipu Pb-Zn deposits in the region (Figure 6, Table 4). The mineralization in the Chipu Pb-Zn deposit indicates the involvement of organic matter [26] and it has been speculated that the large vertical "drift" of the H isotope in the ore-forming fluids of the three deposits may be due to the presence of organic H during the mineralization. The gas in the fluid inclusions from Jinniuchang is mainly CH_4, indicating that organic matter was involved in the mineralization [18]. The organic matter is rich in black carbonaceous argillaceous siltstone from the Yuhucun Formation, carbonaceous shale from the Qiongzhusi Formation, and carbonaceous slate from the Kunyang Group, and may be involved in the mineralization of the Maliping, Jinniuchang, and Laoyingqing deposits.

Table 4. Hydrogen and oxygen isotopic compositions in Maliping, Laoyingqing, Jinniuchang Pb-Zn deposits, and major Pb-Zn deposits in the SYGT.

Deposit	Mineral	Sample Quantity	δD‰	$\delta^{18}O_{fluid}$‰	Source
Maliping	Quartz	7	−98.2~−57.8	6.27–11.07	[19]
Laoyingqing	Quartz	8	−93.9~−70.9	4.69–6.79	[67]
Jinniuchang	Quartz	3	−96.4~−75.5	8.49–8.80	[17]
Huize	Calcite	15	−59.8–43.5	6.9~9.3	[13,68]
Maoping	Calcite	3	−64.0~−35.0	−3.7~−1.1	[69]
Maozu	Sphalerite, fluorite, quartz	3	−78.1~−47.9	−6.7~6.9	[2,70]
Daliangzi	Calcite, sphalerite, quartz	6	−74.6~−40.3	−5.3~3.3	[71]
Tianbaoshan	Sphalerite, quartz	5	−51.2~−47.6	−1.9~3.7	[28,72]
Chipu	Quartz	32	−151.4~−48.3	5.1~8.2	[26]

Therefore, the ore-forming fluids of the three deposits derived from the mixed hydrothermal fluid consisting of deep-source fluid flowing through the deep-fold basement (Kunyang Group) and basin brine that leaches organic matter from the wall rock during its migration process.

6.2.2. Mineral Sources

The Pb isotope composition range in different ore bodies, types, and minerals of the Maliping, Laoyingqing, and Jinniuchang deposits is small, which indicates that the Pb sources are consistent (Table 2). The change rate of normal Pb generally ranges from 0.3 to 1% and the range of the Pb isotope ratios in the three deposits is smaller than 1, indicating a relatively stable Pb source (Table 2) [17,18]. The Pb isotopic compositions of the sulfides in the three deposits are uniform, which may be caused by a (completely) mixed or single Pb source. The Pb isotopic compositions of the sulfides show a linear trend in the $^{208}Pb/^{204}Pb$-$^{206}Pb/^{204}Pb$ diagram (Figure 5b,d,f), which indicates mixed Pb sources [73,74]. The Pb isotopic compositions of all samples from the three deposits in the $^{207}Pb/^{204}Pb$-$^{206}Pb/^{204}Pb$ diagram (Figure 5a,c,e) show an approximate east-west straight line on the average evolution line of Pb in the upper crust, which indicates that Pb ore is mainly derived from the upper crust, with a small orogenic amount.

Considering the extensive exposure of Emeishan basalt and basement rocks (Kunyang and Huili Groups) in the SYGT and that main host rock of the Pb-Zn deposits are carbonate rocks, many scholars believe that the ore-forming materials of the Pb-Zn deposits in the area are jointly provided by the three, but their contributions are different: (1) they are mainly provided by carbonate rocks [13]; (2) they are mainly provided by Precambrian basement rocks [4]; and (3) Emeishan basalt not only provides some ore-forming materials but also provides the main thermal power source [11].

The Pb isotopic content of the ore in the Maliping, Laoyingqing, and Jinniuchang deposits notably differs from that of the area's basalt, Sinian dolomite, and Devonian–Permian carbonate rocks. They are consistent with the basement rocks of the Kunyang Group (Figure 5a,c,e). The Pb isotope compositions of the Maliping deposit plot within the range of basement rocks (Figure 5a), indicating that the metals in the ore-forming fluid of the deposit are mainly provided by basement rocks (Kunyang Group) and that the Pb isotope has undergone homogenization during the ore-forming process. The metals in the ore-forming fluid of the Jinniuchang deposit are consistent with those of the Maliping deposit [18]. The metals in the ore-forming fluid of the Laoyingqing deposit are also derived from the basement rocks (Kunyang Group). Devonian–Permian carbonate rocks and Dengying Formation dolomite also provide a small amount of metal materials and the Pb isotope contents are uniform during the ore-forming process [17]. This notably differs from the main sources of Pb ore in most other Pb-Zn deposits in the SYGT (Figure 5a,c,e).

The results of previous studies suggest that the time frame of the Emeishan basaltic magmatism activity is ~260 Ma, whereas the regional Pb-Zn metallogenic age is ~200 Ma, representing a difference of more than 50 Ma [52,75]. This indicates that there is no direct genetic relationship between them, and it is possible that ore-forming fluids leached some ore-forming metals in the Emeishan basalt during migration [14].

The isotopic dating results show that the ore-forming age of the deposits in the SYGT ranges from Late Triassic to Early Jurassic, with a concentration of ~200 Ma [52]. The Rb-Sr isochron age of sphalerite from the Laoyingqing deposit is 209.8 $\pm$ 5.2 Ma, which is consistent with the latter conclusion [17]. The $^{87}Sr/^{86}Sr$ ratio of the four sphalerite samples from the Maliping deposit ranges from 0.710377 to 0.714149 (mean: 0.712073) after age correction. This mean value is close to but slightly lower than that of the continental crust (mean 0.719) and higher than that of mantle Sr (0.707) [76]. Therefore, it is believed that the ore-forming materials of the deposit are mainly derived from continental crust, which is in good agreement with the Pb isotope tracing results.

Some scholars believe that the Pb-Zn ore-forming fluid in the SYGT may be a mixture of three fluids flowing through the basement rocks, sedimentary rocks of different strata, and Emeishan basalt [11,14,15,41,77]. Based on the comparative analysis in Figure 7, the $(87Sr/86Sr)_{200\ Ma}$ values of the main deposits in the SYGT are notably higher than those of the mantle and Emeishan basalts, indicating that the ore-forming materials cannot be completely provided by the mantle and Emeishan basalts. This is consistent with the previous conclusion that the Emeishan mantle plume cannot contribute many ore-forming materials through numerous geological and geochemical studies [18,78,79]. The $(87Sr/86Sr)_{200\ Ma}$ values of the main deposits in the area are higher than those of Upper Sinian–Permian sedimentary rocks and lower than those of basement rocks, suggesting that the ore-forming minerals are mainly provided by both the sedimentary rocks of the host strata and the basement rocks. The Laoyingqing, Huize, and Daliangzi deposits have higher $(87Sr/86Sr)_{200\ Ma}$ values, indicating that the ore-forming materials are mainly derived from the basement rocks (Kunyang Group). The $(87Sr/86Sr)_{200\ Ma}$ values of the Maliping, Maoping, Shanshulin, Shaojiwan, and Tianqiao deposits are more similar to those of Upper Sinian to Permian carbonate rocks (0.7073–0.7111), indicating that the ore-forming materials mainly derived from marine carbonate rocks.

Therefore, it has been suggested that the Sr in ore-forming fluids of the Maliping and Laoyingqing deposits is derived from a mixture of ore-forming fluids flowing through the basement rocks (Kunyang Group) and sedimentary rocks of the caprock, which are the same as the main deposits in the SYGT.

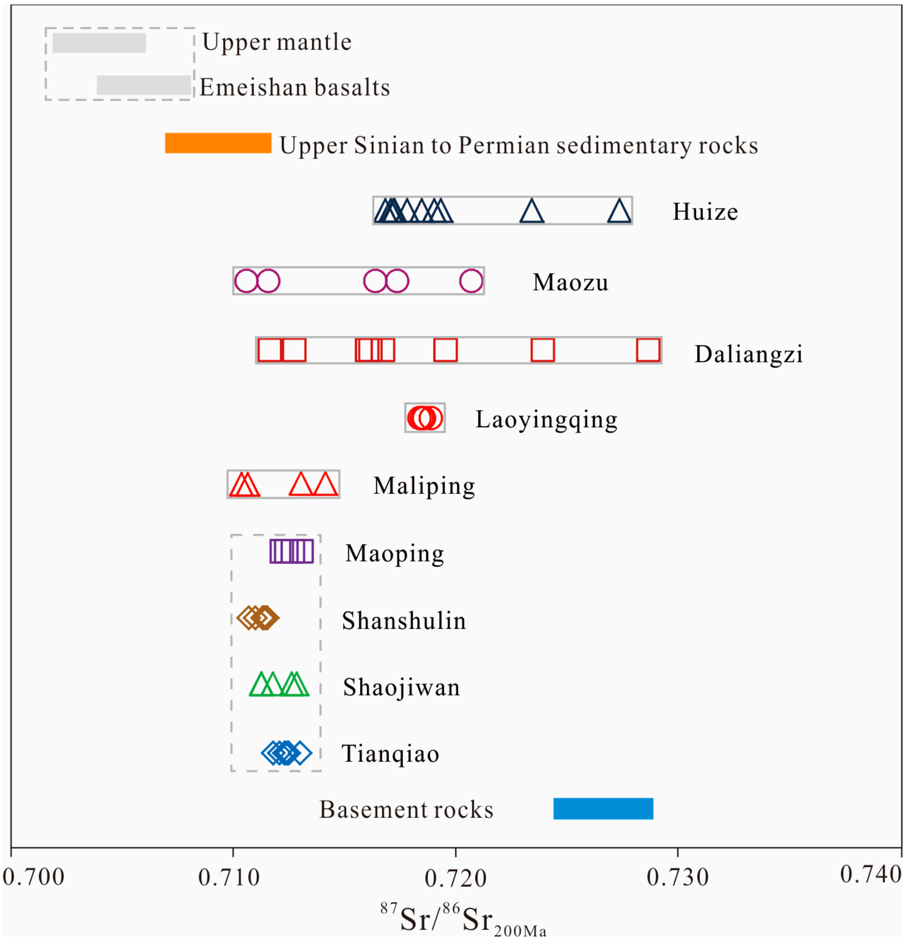

Figure 7. Comparison of($^{87}Sr/^{86}Sr)_t$ (t = 200 Ma) ratios among the major SYGT Pb-Zn deposits, sedimentary rocks, basement rocks, EmeishanBasalts, and upper mantle. (Huize [80]; Maozu [81]; Maoping [82]; Daliangzi [83]; Shanshulin [31,77]; Shaojiwan [32]; Tianqiao [14]; Chipu [26,77]; Upper mantle [76]; Emeishan basalts [11]; Sedimentary rocks [8,9,31,32]; and Proterozoic basement rocks [84,85]).

6.3. Metallogenic Mechanism

The Rb-Sr age of the Laoyingqing deposit is consistent with that of most other Pb-Zn deposits in the SYGT (230–190 Ma), within the error range (Table 5). The Maliping, Laoyingqing, and Jinniuchang deposits have similar mineral compositions, homogenization temperatures, salinities of fluid inclusions, and sources of ore-forming materials and fluids. All ore bodies are vein-like and layered and are controlled by structures belonging to the northeast structural belt system [86]. Furthermore, the three deposits have several characteristics in common with other deposits in the SYGT such as compression structure, ore control by fold and fault-fold structures, notable epigenetic characteristics, simple mineral composition, vein and lenticular orebodies, and a weak relationship with magma (Emeishan mantle plume). The ore-forming fluids of the three deposits are medium-high temperature and medium-low salinity, consistent with the main Pb-Zn deposits in the SYGT (Table 5). Therefore, the three Pb-Zn deposits in clastic rocks in the Dahai mining area may have formed synchronously with other Pb-Zn deposits in the SYGT under a regional hydrothermal event triggered by the Late Indosinian collision orogeny. Their metallogenic dynamic background is related to the closure of the Paleotethys Ocean caused by the collision between the Indosinian and Yangtze blocks in the Indosinian Period (230–200 Ma) [17].

The ore-forming fluid of three Pb-Zn deposits in clastic rocks of the Dahai mining area is mainly derived from the mixed hydrothermal solution of deep-source fluid flowing through the basement (Kunyang Group) and basin brine containing organic matter. Driven by tectonic dynamics, the high-pressure deep-source fluid continues to rapidly migrate upward, which prevents the basin fluid in the stratum from migrating downward along the fault, and it is impossible for the two fluids to flow and mix simultaneously in opposite directions in the fault. Considering that reduced S generation requires a large amount of heat and organic matter, to ensure the simultaneous existence of SO_4^{2-}, organic matter, and thermal energy to generate reduced S, the basin fluid should be migrated to the ore-bearing space in the early stage, and the deep-source fluid follows in the later stage and mixes with the basin fluid for mineralization.

In summary, the metallogenic mechanism of Pb-Zn deposits in clastic rocks in the Dahai mining area is as follows: (1) The formation of the Indosinian orogenic belt and migration of the basin brine: The Paleotetian Ocean closed due to the Indosinian (230–200 Ma) collision and orogeny between the Indosinian and Yangtze blocks and SSW-direction tectonic stress field from the Indosinian Block, forming the Nanpanjiang-Youjiang orogenic belt and the Nanpanjiang foreland basin in the southeastern part of northeast Yunnan. Owing to orogenic uplift gravity, the basin fluid containing organic matter migrated along the carbonate karst and fractures of Cambrian and Sinian strata at a large scale and over long distances, gradually extracting a small amount of major metallogenetic metal ions, such as Pb and Zn, from the siltstone of the Lower Cambrian Qiongzhusi Formation and sulfate from the gypsum salt in marine carbonate of the Lower Cambrian Yuhucun Formation. This led to the formation of medium-high-salinity acidic fluid containing a small amount of ore-forming materials and a large amount of SO_4^{2-}.This fluid filled the detachment fracture zone of the core and SE wing of the Wuxing anticline as well as the tensile space of the fault in the footwall of the Guancangqing fault in the early stage. (2) The formation of a strike-slip fault-fold structural system and ore-rich fluid: With regional tectonic stress conducted into the Yangtze Block, the NE-trending Mile-Shizong deep fault has left oblique strike-slip and the NW-trending Yadu-Ziyun fault exhibits right oblique strike-slip. Owing to the barrier of the ancient land of Kang-Dian, the Xiaojiang, Puduhe, and Lvzhijiang deep faults exhibit a left strike-slip, forming an intracontinental strike-slip fault-fold structure system in the SYGT [87]. Simultaneously, a fault-fold structure composed of the Daibu and Pingqing inverted anticlines and Wuxing anticlines formed in the Dahai mining area. Driven by the NW-SE tectonic stress field, the high-temperature and low-salinity deep-source fluid migrated upward on a large scale along the Xiaojiang, Huize, Qingmenkou, and Daibu faults and gradually extracted major ore-forming metal ions, such as Pb and Zn, from the basement to form medium-salinity fluid rich in ore-forming materials. (3) Fluid mixing, unloading, and tectonic fluid coupling: The medium-salinity fluid rich in ore-forming materials interacted with the structure during its upward migration, which affected the flow rate and discharge of the ore-forming fluid. When the fluid migrated to the detachment fracture zone of the core and SE wing of the Wuxing anticline and the tensile space of fault in the footwall of the Guancangqing fault, its migration speed decreased due to the "barrier layer" and it mixed with the basin fluid. The thermal energy caused by the deep-source fluid led to the pyrolysis of S-bearing organic matter. Subsequently, reduced S was generated and the TSR started, in which SO_4^{2-} in the fluid was converted into H_2S, and reduced S was generated. In a reducing environment, metal sulfides precipitated, and ores formed (Figure 8).

Table 5. Comparison of characteristics between Maliping, Laoyingqing, and Jinniuchang deposits and main Pb-Zn deposits in SYGT.

Deposits	Position	Host Rocks	Pb + Zn Reserves/Grade	Ore-Controlling Structures	Orebody	Salinity (wt.% NaCl)/Th (°C)	Symbiotic Minerals	Ore-Forming Age (Ma) and Test Method	Source
Huize	NE Yunnan	Early Carboniferous dolostone	>5 Mt/25%–30%	NE-trending thrust faults	Stratiform, lenticular	13–18 and 6–12/150–221 and 250–350	Galena, sphalerite, pyrite, arsenopyrite, chalcopyrite, limonite, calcite, dolomite, quartz	Sphalerite Rb-Sr: 223.5 ± 3.9, 226 ± 6.4, 196.3 ± 1.8	[7,22,80]
Maoping		Upper Devonian dolostone and limestone	3 Mt/>25%	Anticline and NW-trending faults	Stratoid, lenticular, vein	0.8–23/200–215 and 260–300	Sphalerite, galena, pyrite, calcite, quartz	Sphalerite Rb-Sr: 321.7±5.8	[7,69,82]
Maozu		Late Sinian dolostone	2 Mt/12%–14%	NE-trending fold	Stratoid	2.8–5.3/153–248	Sphalerite, galena, calcite, dolomite, quartz, fluorite	Calcite Sm-Nd: 196 ±13	[7,24]
Lehong		Late Sinian dolostone	2.4 Mt/>15%	NW-trending faults	Stratoid, lenticular, vein	11.3–14.5/165–229	Sphalerite, galena, pyrite, arsenopyrite, dolomite, quartz	Sphalerite Rb-Sr: 200.9 ± 8.3	[7,26,79]
Maliping		Interface between Early Cambrian siliceous dolomite and clastic rock	>0.5 Mt/ 15.89%	NE-trending anticline	Stratoid, lenticular, large lentil-like	5.6–15.7/220–309	Sphalerite, galena, pyrite, dolomite, calcite, quartz, barite	No data	This paper; [19]
Laoyingqing		Carbonaceous slate of the Middle Proterozoic Kunyang Group	<0.1 Mt/<10%	NE-trending fold	Finely vein	7.2–20.7 /130–275	Sphalerite, galena, pyrite, quartz, calcite	Sphalerite Rb-Sr: 209.8 ± 5.2	[17]
Jinniuchang		Early Cambrian argillaceous siltstone	<0.1 Mt/<10%Pb + Zn	NE-trending fault-fold structure	Vein	6.5~14.0/165–274	Galena, sphalerite, pyrite, calcite, quartz	No data	[18]
Daliangzi	SW Sichuan	Late Sinian dolostone	4.5 Mt/10%–12%	NW-trending faults	Lenticular, vein	18/170–225	Sphalerite, galena, pyrite, chalcopyrite, quartz, calcite, dolomite	Calcite Sm-Nd: 204.4 ± 1.2	[26,34]
Tianbaoshan		Late Sinian dolostone	2.6 Mt/10%–15%	NNE-trending faults	Stratoid, lenticular, vein	12.4–20/157–267	Sphalerite, galena, chalcopyrite, dolomite, calcite, quartz	Zircon U-Pb age of diabase: >166	[28,51]
Chipu		Late Sinian dolostone	0.65 Mt/10.4%	NW-trending faults and NE-trending faults	Stratoid, lenticular	8.5–17/130–250	Sphalerite, galena, pyrite, dolomite, calcite, quartz, asphalt	Bitumen Re-Os: 292.0 ± 9.7, 165.7 ± 9.9	[26,88]
Shanshulin	NW Guizhou	Late Carboniferous dolomitic limestone	>0.5 Mt/>20%	NW-trending thrust faults	Stratoid, vein	<15/150–280	Sphalerite, galena, pyrite, dolomite, calcite	No data	[31,89]
Shaojiwan		Permian and Devonian dolomitic limestone and dolostone	0.5 Mt/15%–20%	NW-trending fold	Stratoid	0.9–17.5/115–170	Sphalerite, galena, pyrite, dolomite, calcite	No data	[32,89]
Tianqiao		Carboniferous dolostone	0.4 Mt/15%–18%	NW-trending fold	Stratoid	9.6–14.2/150–270	Sphalerite, galena, pyrite, dolomite, calcite	Sphalerite Rb-Sr: 191.9 ± 6.9	[14,75]

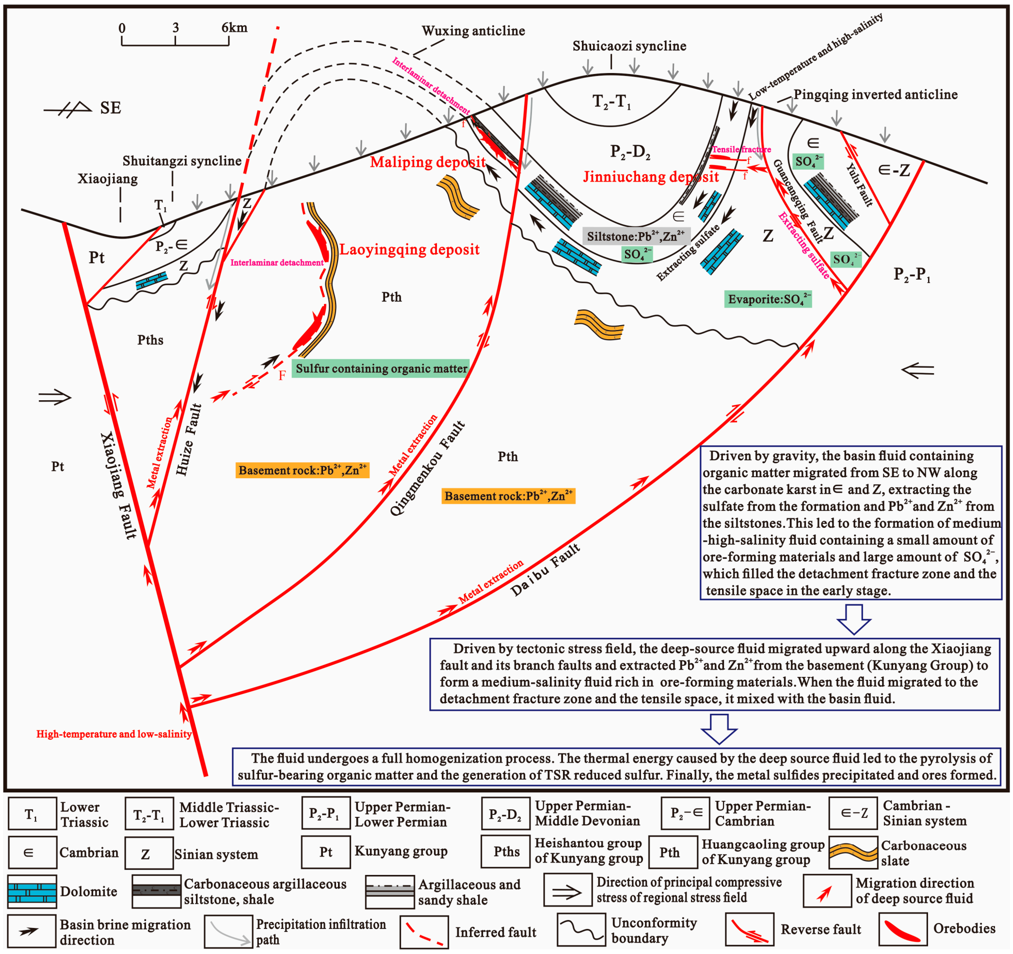

Figure 8. Metallogenic model of Pb-Zn deposits in clastic rocks of Dahai mining area.

7. Conclusions

(1) The ore-forming fluids of the three Pb-Zn deposits in clastic rocks in the Dahai mining area are derived from mixed hydrothermal fluid consisting of deep-source fluid flowing through the deep-fold basement (Kunyang Group) and basin brine that leaches organic matter from the wall rock during its migration process.

(2) The reduced S of the Maliping and Jinniuchang Pb-Zn deposits in clastic rocks is derived from reduced S generated by seawater sulfate by the TSR in the Lower Cambrian Yuhucun and Sinian Dengying formations. The reduced S of the Laoyingqing Pb-Zn deposit is mainly derived from the reduced S generated by the pyrolysis of S-bearing organic matter in the carbonaceous slate of the Kunyang Group. The metals in the ore-forming fluids of the three deposits are derived from basement rocks (Kunyang Group) and a small portion is derived from Devonian–Permian carbonate rocks and dolomite of the Dengying Formation.

(3) The three deposits belong to the same metallogenic system as other major Pb-Zn deposits in the SYGT and formed synchronously with other local Pb-Zn deposits under a regional hydrothermal event triggered by collision orogeny in the Late Indosinian Period (~200 Ma). A unified metallogenic model of Pb-Zn deposits in clastic rocks in the Dahai mining area in which two fluids successively migrate and mix for mineralization is established.

Author Contributions: Conceptualization, H.G. and R.H.; data curation, L.M.; formal analysis, H.G. and G.C.; funding acquisition, R.H.; investigation, H.G. and G.C.; project administration, L.M.; supervision, R.H. and P.W.; writing—original draft, H.G.; writing—review and editing, R.H. and P.W. All authors have read and agreed to the published version of the manuscript.

Funding: This research was financially supported by the National Natural Science Foundation of China (Nos. 42172086 and 41572060), the Yunnan Major Scientific and Technological Projects (No.202202AG050014), the Fund of China Yunling Scholars (2015), the Fund of Mineral Resources Prediction and Evaluation Engineering Laboratory of Yunnan Province in China (2010), and the Fund of Innovation Team of Yunnan Province in China (2012).

Data Availability Statement: Not applicable.

Acknowledgments: I would like to express my gratitude to Wang Shengkai, General Manager of Yunnan Chihong Zinc Germanium Co., Ltd., and Guo Zhonglin, a senior engineer, for their strong support and help with fieldwork.

Conflicts of Interest: The authors declare no conflict of interest.

References

1. Han, R.S.; Hu, Y.Z.; Wang, X.K.; Hou, B.H.; Huang, Z.L.; Chen, J.; Wang, F.; Wu, P.; Li, B.; Wang, H.J.; et al. Mineralisation model of rich Ge-Ag bearing Zn-Pb polymetallic deposit concentrated district in northeastern Yunnan, China. *Acta Geol. Sin.* **2012**, *86*, 280–294. (In Chinese with English Abstract)
2. Liu, H.C.; Lin, W.D. *Regularity Research of Pb-Zn-Ag Ore Deposits Northeastern Yunnan*; Yunnan University Press: Kunming, China, 1999; pp. 1–468. (In Chinese)
3. Chen, S.J. A discussion on the sedimentary origin of Pb-Zn deposits in western Guizhou and northeastern Yunnan. *J. Guizhou Geol.* **1984**, *8*, 35–39. (In Chinese with English Abstract)
4. Zhou, C.X.; Wei, S.S.; Guo, J.Y.; Li, C.Y. The source of metalsin the Qilinchang Zn-Pb deposit, Northeastern Yunnan, China: Pb-Sr isotope constrains. *Econ. Geol.* **2001**, *96*, 583–598. [CrossRef]
5. Zhang, C.Q.; Wu, Y.; Hou, L.; Mao, J.W. Geodynamic setting of mineralization of Mississippi Valley-type deposits in world-class Sichuan-Yunnan-Guizhou Zn-Pb triangle, southwest China: Implications from age-dating studies in the past decade and the Sm-Nd age of Jinshachang deposit. *J. Asian Earth Sci.* **2014**, *103*, 103–114. [CrossRef]
6. Wu, T.; Huang, Z.L.; He, Y.F.; Yang, M.; Fan, H.F.; Wei, C.; Ye, L.; Hu, Y.S.; Xiang, Z.Z.; Lai, C.K. Metal source and ore-forming process of the Maoping carbonate-hosted Pb-Zn deposit in Yunnan, SW China: Evidence from deposit geology and sphalerite Pb-Zn-Cd isotopes. *Ore Geol. Rev.* **2021**, *135*, 104214. [CrossRef]
7. Han, R.S.; Zhang, Y.; Wang, F.; Wu, P.; Qiu, W.L.; Li, W.Y. *The Metallogenic Mechanism of the Germanium-Rich Lead-Zinc Deposit and Prediction of Concealed Ore Location in the Ore Concentration Area of Northeastern Yunnan*; Science Press: Beijing, China, 2019; pp. 1–510. (In Chinese)
8. Hu, Y.G. *Ag Occurrence, Source of Ore-Forming Metals and Mechanism of Yinchangpo Ag-Pb-Zn Deposit, Guizhou*; Institute of Geochemistry, CAS: Guiyang, China, 1999; pp. 10–55. (In Chinese with English Abstract)
9. Deng, H.L.; Li, C.Y.; Tu, G.Z.; Zhou, Y.M.; Wang, C.W. Strontium isotope geochemistry of the Lemachang independent silver ore deposit, northeastern Yunnan. China. *Sci. China Ser. D Earth Sci.* **1999**, *29*, 496–503. (In Chinese with English Abstract) [CrossRef]
10. Tu, S.Y. *The Mineralography Characteristics and its Genetic Significance of the Tianbaoshan Pb-Zn Deposit in Huili Sichuan*; Chengdu University of Technology: Chengdu, China, 2014. (In Chinese with English Abstract)
11. Huang, Z.L.; Chen, J.; Han, R.S. *Geochemistry and Ore-Formation of the Huize Giant Lead-Zinc Deposit, Yunnan Province, China: Discussion on the Relationship between the Emeishan Flood Basalts and Lead-Zinc Mineralization*; Geological Publishing House: Beijing, China, 2004; pp. 1–145. (In Chinese)
12. Zhang, C.Q. The Genetic Model of Mississippi Valley-Type Deposits in the Boundary Area of Sichuan, Yunnan and Guizhou Provinces, China. Ph.D. Thesis, Chinese Academy of Geological Sciences, Beijing, China, 2008; pp. 1–177. (In Chinese with English Abstract)
13. Li, W.B.; Huang, Z.L.; Zhang, G. Sources of the ore metals of the Huize ore field in Yunnan Province: Constrains from Pb, S, C, H, O and Sr isotope geochemistry. *Acta Petrol. Sin.* **2006**, *22*, 2567–2580. (In Chinese with English Abstract)
14. Zhou, J.X.; Huang, Z.L.; Zhou, M.F.; Li, X.B.; Jin, Z.G. Constraints of C-O-S-Pb isotope compositions and Rb-Sr isotopic age on the origin of the Tianqiao carbonate-hosted Pb-Zn deposit, SW China. *Ore Geol. Rev.* **2013**, *53*, 77–92. [CrossRef]
15. Zhou, J.X.; Bai, J.H.; Huang, Z.L.; Zhu, D.; Yan, Z.F.; Lv, Z.C. Geology, isotope geochemistry and geochronology of the Jinshachang carbonate-hosted Pb-Zn deposit, southwest China. *J. Asian Earth Sci.* **2015**, *98*, 272–284. [CrossRef]
16. Lo, C.H.; Chung, S.L.; LEE, T.Y. Age of the Emeishan flood magmatism and relations to Permian-Triassicboundary events. *Earth Planet. Sci. Lett.* **2002**, *198*, 449–458. [CrossRef]
17. Gong, H.S.; Han, R.S.; Wu, P.; Chen, G.; Li, L.J. Constraints of S-Pb-Sr isotope compositions and Rb-Sr isotopic age on the origin of the Laoyingqing noncarbonate-hosted Pb-Zn deposit in the Kunyang Group, SW China. *Geofluids* **2021**, *2021*, 8844312. [CrossRef]

18. Gong, H.S.; Han, R.S.; Wu, P.; Ma, L.; Chen, G. Constraints of fluid inclusion and H-O-S-Pb isotope compositions on the metallogenic model of the Jinniuchang Pb-Zn deposit, SW China. *Chin. J. Nonferrous Met.* **2022**, *32*, 3206–3226. (In Chinese with English Abstract)
19. Yao, Y.S.; Gong, H.S.; Han, R.S.; Zhang, C.Q.; Wu, P.; Chen, G. Metallogenesis and Formation of the Maliping Pb-Zn deposit in Northeastern Yunnan: Constraints from H-O Isotopes, Fluid Inclusions, and Trace Elements. *Minerals* **2023**, *13*, 780. [CrossRef]
20. Yang, H.M.; Liu, C.P.; Cai, H.; Duan, R.C.; Cai, Y.X.; Lu, S.S.; Tan, J.J.; Zhang, L.G.; Li, H.Q. Preliminary Research on the Rb-Sr Dating Mechanism of Sphalerites with Diluted Acid Leachating. *Geol. Miner. Resour. South China* **2017**, *33*, 344–353. (In Chinese with English Abstract)
21. Kong, Z.G.; Wu, Y.; Zhang, F.; Zhang, C.Q.; Meng, X.Y. Sources of ore-forming material of typical Pb-Zn deposits in the Sichuan-Yunnan-Guizhou metallogenic province: Constraints from the S-Pb isotopic compositions. *Earth Sci. Front.* **2018**, *25*, 125–137. (In Chinese with English Abstract)
22. Han, R.S.; Liu, C.Q.; Huang, Z.L.; Chen, J.; Ma, D.Y.; Lei, L.; Ma, G.S. Geological features and origin of the Huize carbonate-hosted Zn-Pb-(Ag) District, Yunnan, South China. *Ore Geol. Rev.* **2007**, *31*, 360–383. [CrossRef]
23. Wang, C.W.; Li, Y.; Luo, H.Y.; Liu, X.L. Genesis of Maoping Pb-Zn deposit in Yunnan Province. *J. Kunming Univ. Sci. Technol. (Sci. Technol.)* **2009**, *34*, 7–11. (In Chinese with English Abstract)
24. Zhou, J.X.; Huang, Z.L.; Yan, Z.F. The origin of the Maozu carbonate-hosted Pb-Zn deposit, southwest China: Constrained by C-O-S-Pb isotopic compositions and Sm-Nd isotopic age. *J. Asian Earth Sci.* **2013**, *73*, 39–47. [CrossRef]
25. Zhang, Y.X.; Wu, Y.; Tian, G.; Shen, L.; Zhou, Y.M.; Dong, W.W.; Zeng, R.; Yang, X.C.; Zhang, C.Q. Mineralisation age and the source of ore-forming material at Lehong Pb-Zn deposit, Yunnan Province: Constraints from Rb-Sr and S isotopes system. *Acta Mineral. Sin.* **2014**, *34*, 305–311. (In Chinese with English Abstract)
26. Wu, Y. *The Age and Ore-Forming Process of MVT Deposits in the Boundary Area of Sichuan-Yunnan-Guizhou Provinces, Southwest China*; China University of Geosciences: Beijing, China, 2013; pp. 1–167. (In Chinese with English Abstract)
27. Yuan, B.; Mao, J.W.; Yan, X.H.; Wu, Y.; Zhang, F.; Zhao, L.L. Sources of metallogenic materials and metallogenic mechanism of Daliangzi ore field in Sichuan Province: Constraints from geochemistry of S, C, H, O, Sr isotope and trace element in sphalerite. *Acta Petrol. Sin.* **2014**, *30*, 209–220. (In Chinese with English Abstract)
28. Zhou, J.X.; Gao, J.G.; Chen, D.; Liu, X.K. Ore genesis of the Tianbaoshan carbonate-hosted Pb-Zn deposit, Southwest China: Geologic and isotopic (C-H-O-S-Pb) evidence. *Int. Geol. Rev.* **2013**, *55*, 1300–1310. [CrossRef]
29. Zhu, C.W.; Wen, H.J.; Zhang, Y.X.; Fan, H.F. Cadmium and sulfurisotopic compositions of the Tianbaoshan Zn-Pb-Cd deposit, Sichuan Province, China. *Ore Geol. Rev.* **2016**, *76*, 152–162. [CrossRef]
30. He, C.Z.; Xiao, C.Y.; Wen, H.J.; Zhou, T.; Zhu, C.W. Zn-S isotopic compositions of the Tianbaoshan carbonate-hosted Pb-Zn deposit in Sichuan, China: Implications for the source of ore components. *Acta Petrol. Sin.* **2016**, *32*, 3394–3406. (In Chinese with English Abstract)
31. Zhou, J.X.; Huang, Z.L.; Lv, Z.C.; Zhu, X.K.; Gao, J.G.; Mirnejad, H. Geology, isotope geochemistry and ore genesis of the Shanshulin carbonate-hosted Pb-Zn deposit, southwest China. *Ore Geol. Rev.* **2014**, *63*, 209–225. [CrossRef]
32. Zhou, J.X.; Huang, Z.L.; Bao, G.P. Geological and sulfur-lead-strontium isotopic studies of the Shaojiwan Pb-Zn deposit, southwest China: Implications for the origin of hydrothermal fluids. *J. Geochem. Explor.* **2013**, *128*, 51–61. [CrossRef]
33. Sangster, D.F. Mississippi Valley-type and SEDEX lead-zinc deposits: A comparative examination. *Inst. Min. Metall. Trans.* **1990**, *99*, B21–B42.
34. Zheng, M.H.; Wang, X.C. Genesis of the Daliangzi Pb-Zn deposit in Sichuan, China. *Econ. Geol. Bull. Soc. Econ. Geol.* **1991**, *86*, 831–846. [CrossRef]
35. Yan, Z.F.; Huang, Z.L.; Xu, C.; Chen, M.; Zhang, Z.L. Signatures of the source for the Emeishan flood basalts in the Ertan area: Pb isotope evidence. *Chin. J. Geochem.* **2007**, *26*, 207–213. [CrossRef]
36. Wang, X.C.; Zheng, Z.R.; Zheng, M.H.; Xu, X.H. Metallogenic mechanism of the Tianbaoshan Pb-Zn deposit, Sichuan. *Chin. J. Geochem.* **2000**, *19*, 121–133. [CrossRef]
37. Wang, J.Z.; Li, Z.Q.; Ni, S.J. Origin of ore-forming fluids of Mississippi Valley type (MVT) Pb-Zn deposits in Kangdian area, China. *Chin. J. Geochem.* **2003**, *22*, 369–376.
38. Wang, C.M.; Deng, J.; Zhang, S.T.; Xue, C.J.; Yang, L.Q.; Wang, Q.F.; Sun, X. Sediment-hosted Pb-Zn deposits in southwest Sanjiang Tethys and Kangdian area on the western margin of Yangtze Craton. *Acta Geol. Sin. (Engl. Ed.)* **2010**, *84*, 1428–1438.
39. Zartman, R.E.; Doe, B.R. Plumbotyectonics-the mode. *Tectonophysics* **1981**, *75*, 135–162. [CrossRef]
40. Zhou, C.X. The source of mineralizing metals, geochemical characterization of ore-forming solution, and metallogenetic mechanism of Qilinchang Zn-Pb deposit, Northeastern Yunnan Province, China. *Bull. Mineral. Petrol. Geochem.* **1998**, *17*, 36–38. (In Chinese with English Abstract)
41. Han, R.S.; Chen, J.; Huang, Z.L.; Ma, D.Y.; Xue, C.D.; Li, Y.; Zou, H.J.; Li, B.; Hu, Y.Z.; Ma, G.S.; et al. *Dynamics of Tectonic Ore-Forming Processes and Localization-Prognosis of Concealed Orebodies—As Exemplified by the Huize Super-Large Zn-Pb-(Ag-Ge) District, Yunnan*; Science Press: Beijing, China, 2006; pp. 1–200.
42. Li, B. *The Study of Fluid Inclusions Geochemistry and Tectonic Geochemistry of Lead-Zinc Deposits: Taking Huize and Songliang Lead-Zinc Deposits for Examples, in the Northeast of Yunnan Province, China*; Kunming University of Science and Technology: Kunming, China, 2010; pp. 1–194. (In Chinese with English Abstract)

43. Zhu, L.M.; Yuan, H.H.; Luan, S.W. A study of isotopic geochemical features and minerogenetic material source of the disu and Daliangzi Pb-Zn deposits, Sichuan. *J. Mineral. Petrol.* **1995**, *15*, 72–79. (In Chinese with English Abstract)
44. Ohmoto, H.; Rye, R.O. *Isotopes of Sulfur and Carbon*, 2nd ed.; Geochemistry of Hydrothermal Ore Deposits; Barnes, H.L., Ed.; Wiley and Sons, Inc.: New York, NY, USA, 1979; 798p.
45. Ohmoto, H. Systematics of sulfur and carbon isotopes in hydrothermal ore deposits. *Econ. Geol.* **1972**, *67*, 551–579. [CrossRef]
46. Zhou, M.F.; Malpas, J.; Song, X.Y.; Robinson, P.T.; Sun, M.; Kennedy, A.K.; Lesher, C.M.; Keays, R.R. A temporal link between the Emeishan large igneous province (SW China) and the end-Guadalupian mass extinction. *Earth Planet. Sci. Lett.* **2002**, *196*, 113–122. [CrossRef]
47. Shellnutt, J.G.; Denyszyn, S.W.; Mundil, R. Precise age determination of mafic and felsic intrusive rocks from the Permian Emeishan large igneous province (SW China). *Gondwana Res.* **2012**, *22*, 118–126. [CrossRef]
48. Shellnutt, J.G. The Emeishan large igneous province: A synthesis. *Geosci. Front* **2014**, *5*, 369–394. [CrossRef]
49. Ali, J.R.; Thompson, G.M.; Zhou, M.F.; Song, X.Y. Emeishan large igneous province, SW China. *Lithos* **2005**, *79*, 475–489. [CrossRef]
50. Saunders, A.D.; Jones, S.M.; Morgan, L.A.; Pierce, K.L.; Widdowson, M.; Xu, Y.G. Regional uplift associated with continental large igneous provinces: The roles of mantle plumes and the lithosphere. *Chem. Geol.* **2007**, *241*, 282–318. [CrossRef]
51. Wang, R.; Zhang, C.Q.; Wu, Y.; Wei, C. Formation age of the diabase dike in the Tianbaoshan Pb-Zn deposit, Sichuan and its relationships with the Pb-Zn mineralisation. *Miner. Depos.* **2012**, *31*, 449–450. (In Chinese with English Abstract)
52. Tang, Y.Y.; Bi, X.W.; Zhou, J.X.; Liang, F.; Qi, Y.Q.; Leng, C.B.; Zhang, X.C.; Zhang, H. Rb-Sr isotopic age, S-Pb-Sr isotopic compositions and genesis of the ca. 200 Ma Yunluheba Pb-Zn deposit in NW Guizhou Province, SW China. *J. Asian Earth Sci.* **2019**, *185*, 104054. [CrossRef]
53. Wang, X.C. Discussion on the ore forming physicochemical conditions of Tianbaoshan lead-zinc deposit in Sichuan. *Acta Geol. Sichuan* **1990**, *10*, 34–42. (In Chinese with English Abstract)
54. Zhang, T.G.; Chu, X.L.; Zhang, Q.R.; Feng, L.J.; Huo, W.G. The sulfur and carbon isotopic records in carbonates of the Dengying Formation in the Yangtze platform, China. *Acta Petrol. Sin.* **2004**, *20*, 717–724. (In Chinese with English Abstract)
55. Shields, G.A.; Strauss, H.; Howe, S.S. Sulphur isotope compositions of sedimentary phosphorites from the basal Cambrian of China:implications for Neoproterozoic–Cambrian biogeochemical cycling. *J. Geol. Soc.* **1999**, *156*, 943–955. [CrossRef]
56. Ohmoto, H. Stable isotope geochemistry of ore deposits. *Rev. Mineral.* **1986**, *16*, 491–560.
57. Machel, H.G.; Krouse, H.R.; Sassen, R. Products and distinguishing criteria of bacterial and thermochemical sulfate reduction. *Appl. Geochem.* **1995**, *10*, 373–389. [CrossRef]
58. Chen, X.; Xue, C.J. Origin of H_2S in Uragen large-scale Zn-Pb mineralisation, western Tian Shan: Bacteriogenic structure and S-isotopic constraints. *Acta Petrol. Sin.* **2016**, *32*, 1301–1314. (In Chinese with English Abstract)
59. Machel, H.G. Bacterial and thermochemical sulfate reduction in diagenetic settings-old and new insights. *Sediment. Geol.* **2001**, *140*, 143–175. [CrossRef]
60. Yuan, S.D.; Chou, I.M.; Burruss, R.C. Disproportionation and thermochemica1 sulfate reduction reactions in S-H_2O-CH_4 and S-D_2O-CH_4 systems from 200 to 340 °C at elevated pressures. *Geochim. Et Cosmochim. Acta* **2013**, *118*, 263–275. [CrossRef]
61. Hu, R.Z.; Fu, S.; Huang, Y.; Zhou, M.F.; Fu, S.; Zhao, C.; Wang, Y.; Bi, X.; Xiao, J. The giant South China Mesozoic low-temperature metallogenic domain: Reviews and a new geodynamic model. *J. Asian Earth Sci.* **2017**, *137*, 9–34. [CrossRef]
62. Zhou, J.X.; Xiang, Z.Z.; Zhou, M.F.; Feng, Y.X.; Luo, K.; Huang, Z.L.; Wu, T. The giant Upper Yangtze Pb-Zn province in SW China: Reviews, new advances and a new genetic model. *J. Asian Earth Sci.* **2018**, *154*, 280–315. [CrossRef]
63. Liu, W.H.; Zhang, J.; Wang, J. Sulfur isotope analysis of carbonate-hosted Zn-Pb deposits in northwestern Guizhou Province, Southwest China: Implications for the source of reduced sulfur. *J. Geochem. Explor.* **2017**, *181*, 31–44. [CrossRef]
64. Zhou, J.X.; Luo, K.; Wang, X.C.; Wilde, S.A.; Wu, T.; Huang, Z.L.; Cui, Y.L.; Zhao, J.X. Ore genesis of the Fule Pb-Zn deposit and its relationship with the Emeishan Large Igneous Province: Evidence from mineralogy, bulk COS and in situ S, Pb isotopes. *Gondwana Res.* **2018**, *54*, 161–179. [CrossRef]
65. Kesler, S.E.; Vennemann, T.W.; Fredeickson, C. Hydrogen and oxygen isotope evidence for origin of MVT-forming brines, southern Appalachians. *Geochim. Et Cosmochim. Acta* **1997**, *61*, 1513–1523. [CrossRef]
66. Sverjensky, D.A.; Rye, D.M. The lead and sulfide isotopic compositions of galena from a Mississippi valley-type deposit in the New lead beIt, Southeast Missouri. *Econ. Geol.* **1979**, *74*, 1491–1543. [CrossRef]
67. Gong, H.S. *Structural Ore-Controlling Characteristics and Metallogenic Mechanism of Lead-Zinc Deposits Clastic Rocks-Hosted in the Dahai Mining Area, Northeast Yunnan*; Kunming University of Science and Technology: Kunming, China, 2022; pp. 1–164. (In Chinese with English Abstract)
68. Guo, X. *Mineralization and Metallogenic Pattern of Lead-Zinc Deposits in Northeast Yunnan*; China University of Geosciences: Beijing, China, 2011; pp. 1–167. (In Chinese with English Abstract)
69. Han, R.S.; Zou, H.J.; Hu, B.; Hu, Y.Z.; Xue, C.D. Features of fluid inclusions and sources of ore-forming fluid in the Maoping carbonate-hosted Zn-Pb-(Ag-Ge) deposit, Yunnan, China. *Acta Petrol. Sin.* **2007**, *23*, 2109–2118.
70. Que, M.Y.; Luo, A.P.; Zhang, L.S. *Upper Sinian and Lower Cambrian Stratified Lead-Zinc Deposits in Northeastern Yunnan*; Chengdu University of science and Technology Press: Chengdu, China, 1993; pp. 1–169. (In Chinese)
71. Yang, Y.X.; Ke, C.X.; Lin, F.C. *Metallogeny of Lead-Zinc Deposit the Eastern Margin of Kangdian Axis*; Sichuan Science and Technology Publishing House: Chengdu, China, 1994; pp. 1–175. (In Chinese)
72. Wang, X.C. Genesis analysis of the Tianbaoshan. *J. Chengdu Coll. Technol.* **1992**, *19*, 10–20. (In Chinese with English Abstract)

73. Canals, A.; Cardellach, E. Ore lead and sulfur isotope pattern form the low-temperature veins of the Catalonian Coastal Ranges (NE Spain). *Miner. Depos.* **1997**, *32*, 243–249. [CrossRef]
74. Kamona, F.A.; Lévêque, J.; Friedrich, G.; Haack, U. Lead isotopes of the carbonate-hosted Kabwe, Tsumeb, and Kipushi Pb-Zn-Cu sulphide deposits in relation to Pan African orogenesis in the Damaran-Lufilian Fold Belt of Central Africa. *Miner. Depos.* **1999**, *34*, 273–283. [CrossRef]
75. Zhou, J.X.; Huang, Z.L.; Zhou, G.F.; Li, X.B.; Ding, W.; Bao, G.P. Trace elements and rare earth elements of sulfide minerals in the tianqiao Pb-Zn ore deposit, Guizhou Province, China. *Acta Geol. Sin.-Engl. Ed.* **2011**, *85*, 189–199.
76. Faure, G. *Principles of Isotope Geology*; John Wiley & Sons: New York, NY, USA, 1986; pp. 183–199.
77. Cheng, P.L.; Xiong, W.; Zhou, G.; He, Z.W. A preliminary study on the origins of ore-forming fluids and their migration directions for Pb-Zn deposits in NW Guizhou Province, China. *Acta Mineral. Sin.* **2015**, *35*, 509–514. (In Chinese with English Abstract)
78. Li, W.B.; Huang, Z.L.; Yin, M. Dating of the giant Huize Zn-Pb ore field of Yunnan Province, Southwest China: Constraints from the Sm-Nd system in hydrothermal calcite. *Resour. Geol.* **2007**, *57*, 90–97. [CrossRef]
79. Mao, J.W.; Zhou, Z.H.; Feng, C.Y.; Wang, Y.T.; Zhang, C.Q. A preliminary study of the Triassic large-scale mineralisation in China and its geodynamic setting. *Geology* **2012**, *39*, 1437–1471. (In Chinese with English Abstract)
80. Yin, M.D.; Li, W.B.; Sun, X.W. Rb-Sr isotopic dating of sphalerite from the giant Huize Zn-Pb ore field, Yunnan Province, Southwestern China. *Chin. J. Geochem.* **2009**, *28*, 70–75. [CrossRef]
81. Zheng, R.H.; Gao, J.G.; Nian, H.L.; Jia, F.J. Rb-Sr isotopic compositions of sphalerite and its geological implications for Maozu Pb-Zn deposit, Northeast Yunnan Province, China. *Acta Mineral. Sin.* **2015**, *35*, 435–438. (In Chinese with English Abstract)
82. Shen, Z.W.; Jin, C.H.; Dai, Y.P.; Zhang, Y.; Zhang, H. Mineralisation age of the Maoping Pb-Zn deposit in the Northeastern Yunnan Province: Evidence from Rb-Sr isotopic dating of sphalerites. *Geol. J. China Univ.* **2016**, *22*, 213–218. (In Chinese with English Abstract)
83. Zhang, C.Q.; Li, X.H.; Yu, J.J.; Mao, J.W.; Chen, F.K.; Li, H.M. Rb-Sr dating of single sphalerites from the Daliangzi Pb-Zn deposit, Sichuan, and its geological significances. *Geol. Rev.* **2008**, *54*, 532–538. (In Chinese with English Abstract)
84. Li, F.H.; Qin, J.M.; Shen, Y.L.; Yu, F.X.; Zhou, G.F.; Pan, X.N.; Li, X.Z. *Presinian System in Kangdian Area*; Chongqing Press: Chongqing, China, 1988.
85. Chen, H.S.; Ran, C.Y. *Geochemistry of Copper Deposit in Kangdian Area*; Geological Publishing House: Beijing, China, 1992.
86. Sun, J.C.; Han, R.S. *Theory and Method of Ore Field Geomechanics*; Science Press: Beijing, China, 2016. (In Chinese)
87. Han, R.S.; Wu, P.; Zhang, Y.; Huang, Z.L.; Wang, F.; Jin, Z.G.; Zhou, G.M.; Shi, Z.L.; Zhang, C.Q. New progresses of metallogenic theory for rich Zn-Pb-(Ag-Ge) deposits in the Sichuan-Yunnan-Guizhou Triangle (SYGT) area, Southwestern Tethys. *Acta Geol. Sin.* **2022**, *96*, 554–573. (In Chinese with English Abstract)
88. Wu, Y.; Zhang, C.Q.; Mao, J.W.; Zhang, W.S.; Wei, C. The relationship between oil-gas organic matter and MVT mineralization: A case study of the chipu lead-zinc deposit, Sichuan. *Acta Geosci. Sin.* **2013**, *34*, 425–436. (In Chinese with English Abstract)
89. Han, R.S.; Wang, M.Z.; Jin, Z.G.; Li, B.; Wang, Z.Y. Ore-controlling mechanism of NE-trending ore-forming structural system at Zn-Pb polymetallic ore concentration area in northwestern Guizhou. *Acta Geol. Sin.* **2020**, *94*, 850–868. (In Chinese with English Abstract)